Cross-Evaluation of Waveform Modulation Schemes Using Post-Experimental Field Data for Underwater Acoustic Communications

Yukang Xue Y. Rosa Zheng, *Fellow, IEEE,*
Dept. of Electrical & Computer Engineering, Lehigh University, Bethlehem, PA 18015

***Abstract*—In this paper, we extend the data dithering reuse (DDR) method to waveform modulation for underwater acoustic (UWA) communications, enabling post-experimental cross-evaluation between single carrier modulation (SCM) and orthogonal frequency division multiplexing (OFDM). The proposed DDR method respectively adds dithering and reverse dithering to the transmitted and received data of the original experimental scheme (OES) thus evaluating the new scheme under test (SUT). We first shows the necessary modifications to the standard testbed of the OES to prepare for DDR at the waveform level of the waveform modulation. We then describe the methods for generating waveform dithering sequences that includes the necessary adjustment to the OES data block that bridges SCM signals of different block lengths with OFDM signals with cyclic prefix (CP) or zero-padding (ZP) guard intervals. Subsequently, we provide a generic framework for multiple-input multiple-output (MIMO) soft-decision frequency-domain turbo equalization (FDTE) compatible with SCM and OFDM. Finally, numerical results using experimental data confirm that the proposed approach can achieve reliable post-experimental cross-evaluation.**

***Index Terms*—cross-evaluation, waveform modulation, single carrier modulation (SCM), orthogonal frequency division multiplexing (OFDM), underwater acoustic (UWA) communications.**

I. Introduction

Underwater acoustic (UWA) communication systems often experience challenging propagation characteristics and complex underwater environment [1]. However, the lack of universally accepted channel models make it difficult to effectively and accurately evaluate the performance of different algorithms using numerical simulations. Researchers in this field therefore tend to test their algorithms through field experiments which are often expensive and time-consuming, requiring significant cost and preparation.

Although computer-generated Wide-sense stationary uncorrelated scattering (WSSUS) channel models are widely accepted in terrestrial RF communications [2], the difficulties encountered in numerical simulation of acoustic communication channels include the nonlinearity and wide-sense non-stationality of acoustic propagation as almost all available channel models [3]–[6] assume the wide-sense stationary property by specifying spatial-temporal correlation, and the linearity by using convolution to describe the channel input and output relationship. These assumptions are often differ from the reality thus resulting in unrealistically great performance of the scheme under test (SUT). recently, a hybrid replay approach incorporates the measured channel impulse response (CIR) from real-world experiments into the simulation testbed and compares different SUTs in a quasi-realistic environment [7], [8]. These methods can well describe the time-varying linear convolution process on fine time scales, but still suffer from the loss of the nonlinear and non-stationary components associated with the actual passband UWA channels. Therefore, the hybrid channel replay methods still predict overly optimistic performance over field experimental studies.

More recently, a data dithering reuse (DDR) method [9], [10] utilizes the post-experimental data and preserves their experience of the real-world acoustic channel to evaluate different forward error correction (FEC) coding and different bit-to-symbol mapping schemes. This approach provides enormous opportunities to existing experimental data, especially those that have failed to perform well can now be dithered to lower constellation orders or stronger error correction codes. The performance of the SUT is shown to preserve the fidelity of the field experiments and is more trustworthy than the channel replay or computer simulated channel models. The dithering of different coding schemes is referred to as bit dithering reuse and the evaluation of different symbol mapping schemes is referred to as constellation dithering reuse.

In this paper, we extend the DDR method for post-experimental evaluation of SUTs beyond FEC and symbol mapping, i.e., waveform modulation schemes and for multiple-input multiple-output (MIMO) [11] systems. The proposed waveform dithering reuse method implements a post-experimental cross-evaluation between single carrier modulation (SCM) and orthogonal frequency division multiplexing (OFDM), thus enabling the cross evaluation of channel estimation and channel equalization of the SCM and OFDM. The waveform DDR can be combined with the bit and constellation DDR, but the fidelity of the SUT performance depends on the channel estimation and equalization methods used.

Specifically, we present the details for how to generate the waveform dithering sequence between the OES and SUT data blocks when the SCM signals have different block lengths and the OFDM signals use cyclic prefix (CP) or zero-padding (ZP) guard intervals. We provide a generic framework for SCM and OFDM compatible MIMO soft decision frequency domain turbo equalization (FDTE) and analyze the equivalent channel models. Finally, numerical results using the undersea 2008 Surface Processes and Acoustic Communications Experiment

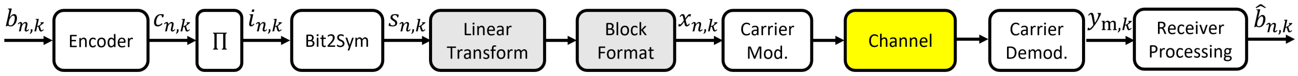

Fig. 1: Signal flow for uniform system model of SCM and OFDM

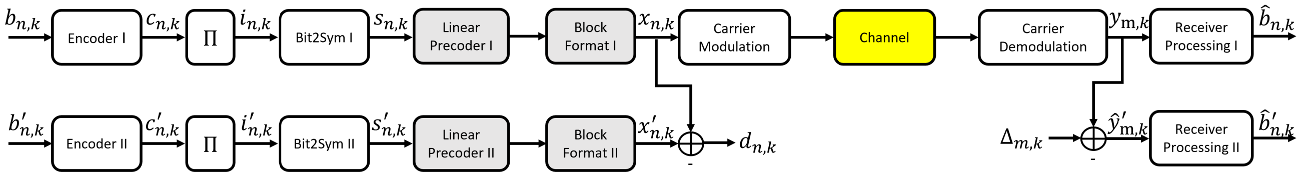

Fig. 2: Data dithering reuse signal flow

(SPACE08) data confirm that the proposed waveform DDR approach enables reliable post-experimental cross-evaluation.

II. System Model

In this section, we unify the system models of SCM and OFDM by introducing a precoder and a block formatter, as shown in Fig. 1, where n, m, k denote the transmitter, receiver, and time indices, respectively. The $N \times M$ MIMO UWA communication system has N projectors and M hydrophones, and the data block length of $x_{n,k}$ is K. The information bit stream $b_{n,k}$ of the nth projector at time instant k is independently encoded (Encoder), interleaved (Π), and mapped (Bit2Sym), where $c_{n,k}$, $i_{n,k}$, $s_{n,k}$ denote the encoded bit, the interleaved bit and the mapped symbol, respectively. The mapped baseband symbols $s_{n,k}$ are precoded and formatted into the baseband waveform streams $x_{n,k}$, $n = 1, \cdots, N$ and $k = 1, \cdots, K$. For the SCM, the Linear transform is simply an identity matrix with a block size of K for each n, and the block formatter may insert guard interval or CP/ZP if needed. For the OFDM, the Linear transform is the K-point inverse fast Fourier transform (IFFT) matrix for each n, and the block formatter is the CP or ZP insertion. The waveform modulated signal $x_{n,k}$ is modulated onto the carrier frequency and is sent over the UWA channel. The received signal is then carrier demodulated and fed to the baseband processing. The details of the receiver baseband processing are omitted in the figure, which usually include channel estimation, channel equalization, demodulation and decoding algorithms.

The equivalent baseband signal of the mth hydrophone at time instant k is expressed as

$$y_{m,k} = g_{n,m}(x_{n,k}) + z_{m,k} \tag{1}$$

where $g_{n,m}(\cdot)$ is the end-to-end response of the channel including any amplifiers, signal conditioning, and UWA channel effects, and $z_{m,k}$ is the zero mean additive Gaussian noise (AWGN) whose power is assumed to be σ_z^2. Considering a simplified linear time-varying flat fading channel, then the input-output relationship becomes

$$y_{m,k} = \sum_{n=1}^{N} \sum_{l=0}^{L-1} h_{m,n}^{k,l} x_{n,k-l} + z_{m,k} \tag{2}$$

where L is the channel length, $\{h_{n,m}^{k,l}\}_{l=0}^{L-1}$ is the lth tap of the time-varying impulse response (TVIR) of the channel between the nth projector and the mth hydrophone at time instant k. We can judiciously split the data block to guarantee that the partitioned subblock is shorter than the equivalent channel coherence time, therefore, $h_{m,n}^{k,l} \approx h_{m,n}^{(l)}$. After the inter-block interference (IBI) is removed from the current signal block, the equivalent input and output (I/O) system model for MIMO is defined in vector format as

$$\mathbf{y}_k = \mathbf{H}_k \mathbf{x}_k + \mathbf{z}_k. \tag{3}$$

Where $\mathbf{y}_k \in \mathcal{C}^{M\times 1}$, $\mathbf{x}_k \in \mathcal{C}^{N\times 1}$, $\mathbf{z}_k \in \mathcal{C}^{M\times 1}$, and $\mathbf{H}_k \in \mathcal{C}^{M\times (NL)}$.

Figure 2 illustrates the waveform DDR signal flow, which achieves cross evaluation between SCM and OFDM with post-experimental data. In parallel to the OES data flow, the SUT information bit stream $b'_{n,k}$ is encoded (Encoder II), interleaved (Π), and mapped (Bit2Sym II) to $c'_{n,k}$, $i'_{n,k}$, $s'_{n,k}$, respectively. The channel coding and symbol mapping of SUT and OES can be the same or different. But since OES and SUT use different waveform modulation methods, their Linear transforms and block formatters are different for sure. After the linear precoding and block formatting of SUT, $x'_{n,k}$ is obtained. Therefore, the dithering sequence is generated as $d_{n,k} \triangleq x_{n,k} - x'_{n,k}$. Next, keeping the transmitted waveform unchanged, we approximate the received signal $\hat{y}'_{m,k}$ of the SUT by the received signal $y_{m,k}$ of the OES. At the receiver side, the reverse dithering operation is used to yield $\hat{y}'_{m,k} = y_{m,k} - \Delta_{m,k}$. Note that the reverse dithering operation is done earlier in the receiver side for waveform DDR than for bit and constellation DDR in [10]. Thus the reverse dithering sequence $\Delta_{m,k}$ must be incorporated into the equalizer. The relationship between the dither sequence $d_{n,k}$ and the reverse dither sequence $\Delta_{m,k}$ will be discussed in Section IV.

III. Signal Preparation for Dithering

In this section, we illustrate the preparation of SCM and OFDM data blocks before dithering and interconversion. In general, the SCM data blocks size K_{scm} is larger than that of OFDM, K_{ofdm}. To fit each other's block size, the SCM data block needs to be partitioned into several data subblocks of size K_{sb} to ensure that $K_{sb} = K_{ofdm}$, or the OFDM data block needs to be concatenated to get an extended data block of size K_{cb} to guarantee $K_{cb} = K_{scm}$. Meanwhile, brute force block partition or concatenation can induce inter-block interference (IBI), so we first discuss block extension and truncation methods without leading to IBI.

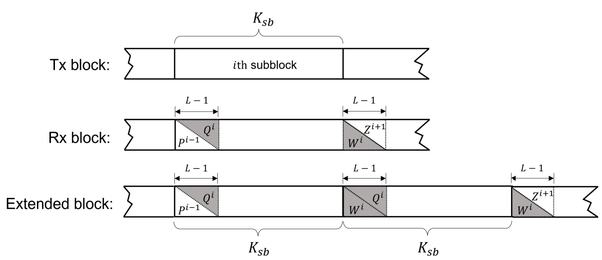

Fig. 3: Block extension

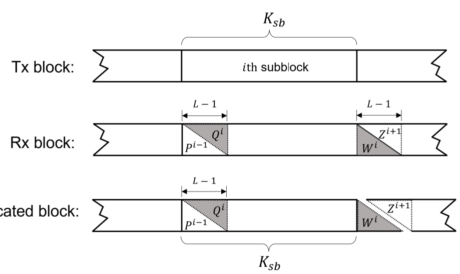

Fig. 4: Block truncation

A. Block extension and truncation

Block extension refers to reusing sub-blocks or combining multiple sub-blocks, and block truncation refers to using a sub-block in the middle position as the end of a block and discarding all sub-blocks after that sub-block. As shown in Fig. 3, we name the interference of the previous $(i-1)$th subblock to the current ith subblock as pre-cursor interference $P_{m,k}^{i-1}$, and the interference of the current ith subblock to the next $(i+1)$th subblock as post-cursor interference $W_{m,k}^{i}$. In block extension and truncation, avoiding IBI is the reconstruction and removal of pre-cursor and post-cursor interference. With a channel length of L, the length of pre-cursor and post-cursor interference is $L-1$, which means that the first $L-1$ and last $L-1$ symbols of each sub-block are related to the interference. The pre-cursor interference from the $(i-1)$th subblock to the ith subblock is reconstructed as

$$P_{m,k}^{i-1} = \sum_{n=1}^{N} \sum_{l=k+1}^{L-1} \hat{h}_{m,n}^{i-1}(l) x_{n,K_{sb}-l+k}^{i-1} \tag{4}$$

where $x_{n,K_{sb}-l+k}^{i-1}$ is the $(K_{sb}-l+k)$th symbol of the $(i-1)$th subblock

$$\mathbf{x}_n^{i-1} = [x_{n,0}^{i-1}, x_{n,1}^{i-1}, \cdots, x_{n,k_{sb}-1}^{i-1}]^T \tag{5}$$

and $\hat{h}_{m,n}^{i-1}(l)$ is the lth estimated channel tap corresponding to the (n,m)th channel link. By removing the pre-cursor interference $P_{m,k}^{i-1}$ from the current subblock $y_{m,k}^{i}$, we get

$$Q_{m,k}^{i} = y_{m,k}^{i} - P_{m,k}^{i-1}, \text{ for } 0 \leq k \leq L-2 \tag{6}$$

where $Q_{m,k}^{i}$ is the first $L-1$ symbols of the ith received subblock $y_{m,k}^{i}$.

Similarly, the reconstructed post-cursor interference $W_{m,k}^{i}$ from the i th subblock to the $(i+1)$ subblock is given

$$Z_{m,k}^{i+1} = \sum_{n=1}^{N} \sum_{l=0}^{k} \hat{h}_{m,n}^{i+1}(l) x_{n,k-l}^{i+1} \tag{7}$$

$$W_{m,k}^{i} = y_{m,k}^{i+1} - Z_{m,k}^{i+1}, \text{ for } 0 \leq k \leq L-2 \tag{8}$$

Where $Z_{m,k}^{i+1}$ is the first $L-1$ symbols of the $(i+1)$th subblock $y_{m,k}^{i+1}$.

Given $P_{m,k}^{i-1}$, $Q_{m,k}^{i}$, $Z_{m,k}^{i+1}$, $W_{m,k}^{i}$, the refined ith subblock is ready to be extended or truncated. Fig. 3 illustrates a block extension method that reuses the ith subblock. The $L-1$ symbol at the splice is obtained by adding $W_{m,k}^{i}$ and $Q_{m,k}^{i}$, which simulates the IBI that exists between neighboring subblocks. Fig. 4 shows the block truncation technique with the ith subblock as the end, using $W_{m,k}^{i}$ as the final tail.

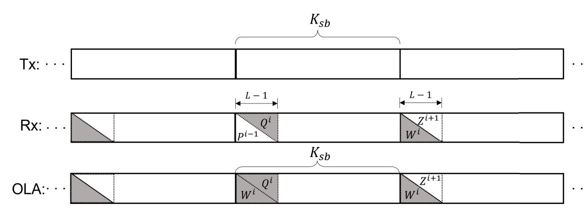

Fig. 5: SCM without gap to OFDM conversion

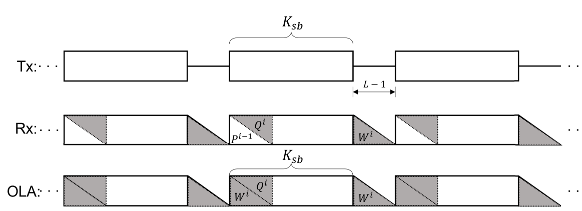

Fig. 6: SCM with gap to OFDM conversion

B. OFDM guard interval (CP/ZP)

OFDM schemes use CP/ZP to eliminate IBI, which is not normally used by SCM schemes. Therefore, bridging the difference between SCM and OFDM data formats regarding the guard interval CP/ZP is another issue we have to deal with. Two steps should be performed to solve this problem: 1) reconstruct and remove the pre-cursor and post-cursor interference induced by the previous and next subblocks; 2) shuffle the tails of the current block and perform overlap adding (OLA). Performing OLA to SCM signals brings another benefit: it convert the equivalent channel response matrix $\mathbf{H}_{m,n}$ into a circulant matrix, making it ideal for frequency domain equalizer design. Fig. 5 and Fig. 6 illustrate how to convert SCM data blocks with or without guard interval into standard OFDM data blocks. Fig. 5 shows the case that there is no gap between blocks when SCM data is transmitted. As a result, the received signals have pre-cursor and post-cursor interference of length $L-1$. To reconstruct and remove the IBI, $P_{m,k}^{i-1}$, $Q_{m,k}^{i}$, $Z_{m,k}^{i+1}$, $W_{m,k}^{i}$ are calculated by equation (4) (6) (7) (8). By removing the pre-cursor interference $P_{m,k}^{i-1}$ and post-cursor interference $Z_{m,k}^{i+1}$, we get the response of the first $L-1$ symbols and the response of the last $L-1$ symbols of the ith sub-block: $Q_{m,k}^{i}$ and $W_{m,k}^{i}$, respectively. By overlap adding $W_{m,k}^{i}$ on $Q_{m,k}^{i}$, the refined head frame of ith subblock is given

$$y_{m,k}^{i} = W_{m,k}^{i} + Q_{m,k}^{i}, \text{ for } 0 \leq k \leq L-2. \tag{9}$$

Thus, the ith subblock is ready to be dithered and converted to the OFDM subblock.

When there is an guard interval of length not less than $L-1$ between the transmitted blocks, adjacent subblocks does not have IBI, i.e., $P_{m,k}^{i-1} = Z_{m,k}^{i+1} = 0$. In this case, $Q_{m,k}^{i}$ is directly treated as the first $L-1$ symbol response of the ith subblock and $W_{m,k}^{i}$ is the $L-1$ length tail. The same OLA operation in equation (9) is performed to complete the block format preparation before dithering. Fig. 6 illustrates the case when the length of the guard interval is exactly $L-1$.

IV. Cross Evaluation

In this section, we provide a generic framework for MIMO soft-decision frequency-domain turbo equalization compatible with SCM and OFDM. Based on the FDTE, we derive the relationship between the dithering sequence $d_{n,k}$ and the reverse dithering sequence $\Delta_{m,k}$ and use them to complete the cross evaluation of SCM and OFDM. Two important assumptions support the implementation.

Remark 1: When the block time duration of SUT is less than the channel coherence time of OES, the channel impulse response within one block duration is treated as time-invariant. This assumption is approximately reached by precisely choosing the block size of SUT.

Remark 2: The mathematical framework of SUT ignores the Doppler effect, where we assume the Doppler component matrix is perfectly recovered and eliminated at the original receiver side of OES. This relaxation leads to no significant performance degradation based on our experimentally numerical result.

In the following, we cross-evaluate SCM and OFDM and derive the relationship between $d_{n,k}$ and $\Delta_{m,k}$. First, we consider the original experimental scheme with OFDM (OES-OFDM) and the data dithering reusing for single-carrier modulation (DDR-SCM). Therefore, the Linear transform II in Fig. 2 is a diagonal matrix, i.e, $x'_{n,k} = s'_{n,k}$. Given the original experimental scheme with SCM (OES-SCM), the data dithering reuse scheme is an OFDM system (DDR-OFDM). The Linear transform II is an IFFT matrix in this case, i.e, $x'_{n,k} = \mathbf{F}_N^H s'_{n,k}$. Since waveform DDR adds dithering sequence $d_{n,k}$ to x instead of s, the above two cases can be discussed under the same framework.

Combining equation (1) and the definitions of $d_{n,k}$ and $\Delta_{m,k}$ in Section II, we have

$$\mathbf{y}^{'} = \mathbf{y} - \mathbf{\Delta} = \mathbf{g}(\mathbf{x}) + \mathbf{z} - \mathbf{\Delta} = \mathbf{g}(\mathbf{x}^{'} + \mathbf{d}) + \mathbf{z} - \mathbf{\Delta} \tag{10}$$

Compared with the target $\mathbf{y}^{'} = \mathbf{g}(\mathbf{x}^{'}) + \mathbf{z}$, we obtain

$$\mathbf{\Delta} = \mathbf{g}(\mathbf{x}) - \mathbf{g}(\mathbf{x}^{'}) = \mathbf{g}(\mathbf{x}^{'} + \mathbf{d}) - \mathbf{g}(\mathbf{x}^{'}) \tag{11}$$

If linear channel described is considered, similar to equation 10, we have

$$\mathbf{y}^{'} = \mathbf{y} - \mathbf{\Delta} = \mathbf{H}\mathbf{x} + \mathbf{z} - \mathbf{\Delta} = \mathbf{H}(\mathbf{x}^{'} + \mathbf{d}) + \mathbf{z} - \mathbf{\Delta} \tag{12}$$

Compared with the target $\mathbf{y}^{'} = \mathbf{H}\mathbf{x}^{'} + \mathbf{z}$, we obtain $\mathbf{\Delta} = \mathbf{H}\mathbf{d}$ which contains all the dithering information that is used to reform the signal of the SUT-SCM under this channel assumption. The characteristic of circulant channel matrix still holds via the linear operation. Comparing $\mathbf{\Delta} = \mathbf{H}\mathbf{d}$ with equation (11) shows that the two are closer as the channel has more linear statistics. Therefore, the error of waveform DDR comes from the nonlinear effects received by the dithering sequence as it passes through the channel, and its advantage comes from preserving the whole response of the original transmission sequence as it passes through the channel. The performance of an equalizer that can combat the effects of channel nonlinearity can improve the accuracy of waveform DDR cross evaluation.

V. Experimental Results

The post-experimentally cross evaluation approach was tested by using the data collected in undersea 2008 Surface Processes and Acoustic Communications experiment. Many details of SPACE08 have been provided in [12]–[14], and we will not repeat the tedious experimental specification for the sake of brevity. Specifically, we chose QPSK and 16QAM modulated SCM signals to implement cross evaluation with OFDM signals. The transmission frame structure is depicted in Fig. 7. An example of received signals is shown in 8

We focused on the 2×12 MIMO scheme, where 30 S3, S4 files (200-m transmission distance) and 25 S5, S6 files (1000-m transmission distance) were processed for the original SCM scheme (OES-SCM) and new OFDM scheme under test (DDR-OFDM); 19 S3, S4 files (200-m transmission distance) and 15 S5, S6 files (1000-m transmission distance) were processed for the original OFDM scheme (OES-OFDM) and new SCM scheme under test (SUT-SCM). Therefore, we obtained two sets of cross comparisons: OES-SCM and DDR-SCM; OES-OFDM and DDR-OFDM. Fig. 9 shows the BER performance of the cross evaluation using the proposed FDTE framework. By observing all the figures, some conclusions are drawn: 1) schemes with small block size performed better than that of schemes with large block size; 2) the comparison results are consistent at different channel lengths and different block lengths; 3) high PAPR of the OES-OFDM dataset make the DDR-SCM have more performance degradation than the OES-SCM.

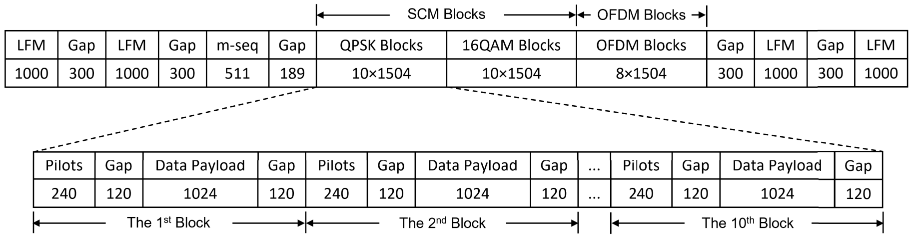

Fig. 7: The selected data structure of SCM and OFDM schemes in the SPACE08 experiment.

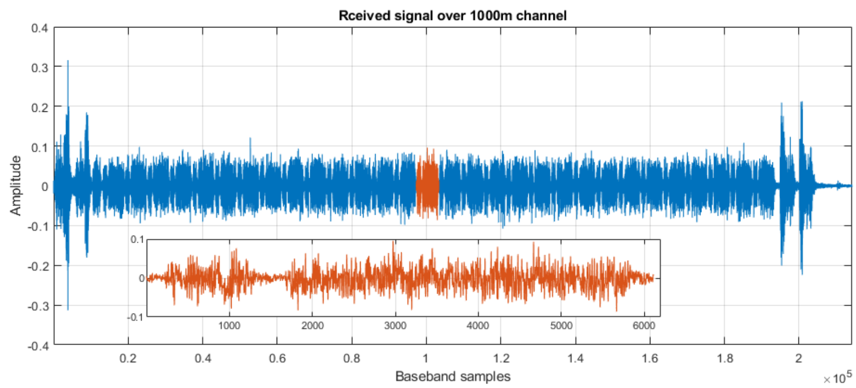

Fig. 8: Example of the received signals in 1000 m transmission.

VI. Conclusion

This paper extends the DDR method to waveform modulation. We introduce signal block preparation, dithering sequence generation, cross evaluation, and also provide a generic framework for MIMO FDTE compatible with SCM and OFDM. Numerical results using experimental data confirm that the proposed approach can achieve reliable post-experimental cross-evaluation.

Acknowledgment

References

[1] D. B. Kilfoyle and A. B. Baggeroer, "The state of the art in underwater acoustic telemetry," *IEEE Journal of oceanic engineering*, vol. 25, no. 1, pp. 4–27, 2000.

[2] C. Xiao, J. Wu, S.-Y. Leong, Y. R. Zheng, and K. B. Letaief, "A discrete-time model for spatio-temporally correlated mimo wssus multipath channels," in *2003 IEEE Wireless Communications and Networking, 2003. WCNC 2003.*, vol. 1. IEEE, 2003, pp. 354–358.

[3] M. B. Porter, "The bellhop manual and user's guide: Preliminary draft," *Heat, Light, and Sound Research, Inc., La Jolla, CA, USA, Tech. Rep*, vol. 260, 2011.

[4] J. C. Peterson and M. B. Porter, "Ray/beam tracing for modeling the effects of ocean and platform dynamics," *IEEE Journal of Oceanic Engineering*, vol. 38, no. 4, pp. 655–665, 2013.

[5] P. Qarabaqi and M. Stojanovic, "Statistical characterization and computationally efficient modeling of a class of underwater acoustic communication channels," *IEEE Journal of Oceanic Engineering*, vol. 38, no. 4, pp. 701–717, 2013.

[6] M. S. Caley and A. J. Duncan, "Wide-band shallow acoustic channel simulation with realistic doppler and delay spreading for 3d evolving rough surfaces," in *2016 IEEE Third Underwater Communications and Networking Conference (UComms)*. IEEE, 2016, pp. 1–5.

[7] R. Otnes, P. A. van Walree, and T. Jenserud, "Validation of replay-based underwater acoustic communication channel simulation," *IEEE Journal of Oceanic Engineering*, vol. 38, no. 4, pp. 689–700, 2013.

[8] P. A. van Walree, F.-X. Socheleau, R. Otnes, and T. Jenserud, "The watermark benchmark for underwater acoustic modulation schemes," *IEEE Journal of Oceanic Engineering*, vol. 42, no. 4, pp. 1007–1018, 2017.

[9] G. Deane, J. Preisig, and A. C. Singer, "Making the most of field data to support underwater acoustic communications r&d," in *2018 Fourth Underwater Communications and Networking Conference (UComms)*. IEEE, 2018, pp. 1–5.

[10] S. Yang, G. B. Deane, J. C. Preisig, N. C. Sevüktekin, J. W. Choi, and A. C. Singer, "On the reusability of postexperimental field data for underwater acoustic communications r&d," *IEEE Journal of Oceanic Engineering*, vol. 44, no. 4, pp. 912–931, 2019.

[11] J. Ling, K. Zhao, J. Li, and M. Lundberg Nordenvaad, "Multi-input multi-output underwater communications over sparse and frequency modulated acoustic channels," *The Journal of the Acoustical Society of America*, vol. 130, no. 1, pp. 249–262, 2011.

[12] X. Qin, F. Qu, and Y. R. Zheng, "Bayesian iterative channel estimation and turbo equalization for multiple-input–multiple-output underwater acoustic communications," *IEEE Journal of Oceanic Engineering*, vol. 46, no. 1, pp. 326–337, 2020.

[13] J. Tao, Y. R. Zheng, C. Xiao, and T. Yang, "Robust mimo underwater acoustic communications using turbo block decision-feedback equalization," *IEEE Journal of Oceanic Engineering*, vol. 35, no. 4, pp. 948–960, 2010.

[14] Z. Yang and Y. R. Zheng, "Iterative channel estimation and turbo equalization for multiple-input multiple-output underwater acoustic communications," *IEEE Journal of Oceanic Engineering*, vol. 41, no. 1, pp. 232–242, 2015.

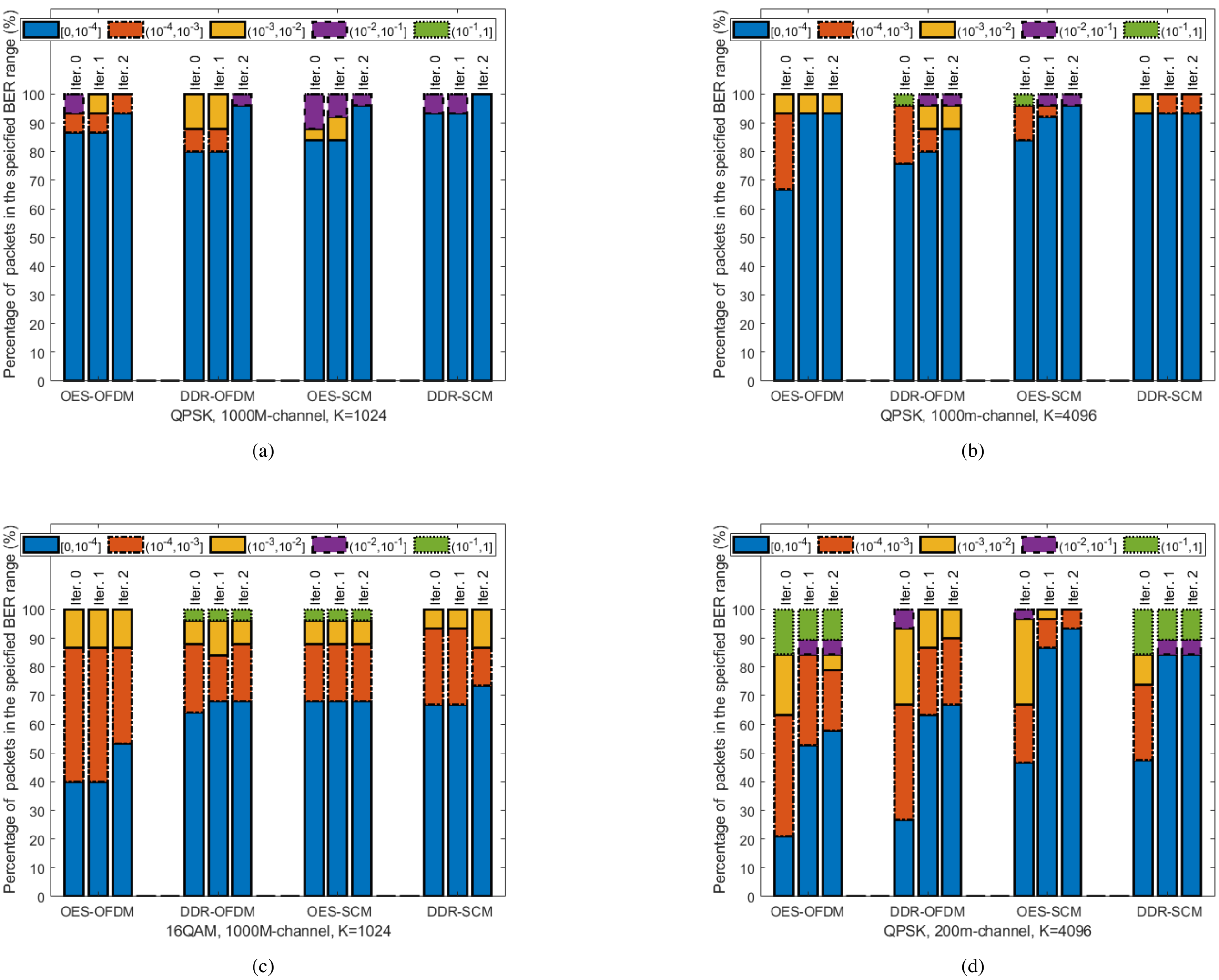

Fig. 9: Results of BER comparison between OES and SUT.